Catalysis Today 166 (2011) 79–83

Contents lists available at ScienceDirect

Catalysis Today

journal homepage: www.elsevier.com/locate/cattod

Effect of crystallization mode of hydrous zirconia support on the isomerization activity of $Pt/WO_3–ZrO_2$

Yueqin Song[a], Juanjuan Zhang[a], Yifei Zhang[a], Xiaolong Zhou[a,*], Jin-An Wang[b], Longya Xu[c]

[a] Petroleum Processing Research Center, East China University of Science and Technology, No. 130, Meilong Road, Shanghai 200237, PR China
[b] Laboratorio de Catálisis y Materiales, ESIQIE, Instituto Politécnico Nacional, Col. Zacatenco, 07738 México, D.F., Mexico
[c] State Key Laboratory of Catalysis, Dalian Institute of Chemical Physics, the Chinese Academy of Sciences, Dalian, Liaoning 116023, PR China

ARTICLE INFO

Article history:
Available online 5 July 2010

Keywords:
Crystallization mode
Hydrous zirconia
Platinum
Tungstated zirconia
Isomerization

ABSTRACT

A series of crystalline hydrous zirconia supports were prepared by different methods. The effects of preparation method of crystalline hydrous zirconia on its crystallization mode and the catalytic activity of $Pt/WO_3–ZrO_2$ in *n*-hexane isomerization were studied. The catalysts were characterized by XRD and Raman spectroscopy, H_2-TPR and NH_3-TPD in order to investigate the crystalline structure, reduction properties and acidity of the catalyst. The results indicated that the crystallization mode of hydrous zirconia from different preparation methods was closely related to the ambience of the process, which significantly influenced the isomerization activity of $Pt/WO_3–ZrO_2$. The crystallization occurring at the surface region of the hydrous zirconia particles led to an inactive $Pt/WO_3–ZrO_2$, while the crystallization occurring only inside hydrous zirconia particles led to a catalyst with high activity.

1. Introduction

Since Hino and Arata found that amorphous hydrous zirconia promoted with W (denoted as $WO_3–ZrO_2$) after calcination at high temperature possessed the strong acidity and isomerization activity of *n*-alkanes [1], tungstated zirconia with or without Pt-promotion as the catalyst for the isomerization reaction of *n*-alkanes attracted much attention [2–11]. Most publications have focused the physicochemical properties and catalytic performances of tungstated zirconia from zirconium hydroxide because this preparation process was generally considered to generate the catalyst with high catalytic activity. Yori et al. [1,2,12] reported that crystallized zirconia support led to an inactive tungstated zirconia catalyst. However, Lebarbier et al. [13,14] compared the catalytic activity of tungstated zirconia from zirconium hydroxide and zirconia (65% tetragonal phase) and found that the two series of the catalysts showed the similar activity. The investigation from Huang et al. [15] revealed that $WO_3–ZrO_2$ showed high *n*-alkane conversion activity when tetragonal zirconia prepared by supercritical drying was used as support. Furthermore, the recent investigations from us and other researchers indicated that $Pt/WO_3–ZrO_2$ from hydrothermal method also exhibited high catalytic activity in *n*-alkane isomerization although crystalline hydrous zirconia acted as support [16,17]. Maybe, the preparation method of crystalline hydrous zirconia may also play an important role in determining the isomerization activity of catalyst except for the crystalline structure of hydrous zirconia support. Unfortunately, the effect of the preparation method of crystalline hydrous zirconia on the isomerization activity of tungstated zirconia has been seldom investigated. The objective of the present work was to investigate the effect of the preparation method of crystalline hydrous zirconia support on the isomerization activity of $Pt/WO_3–ZrO_2$. The crystallization process of $Zr(OH)_4$ in preparation process has been found to strongly depend on the thermal treatment condition and to greatly influence the isomerization activity of the catalyst.

2. Experimental

2.1. Preparation of hydrous zirconia support and catalysts

A series of crystalline hydrous zirconia supports were prepared by several methods. The hydrogel of $Zr(OH)_4$ was prepared by the precipitation method with ammonium solution. $ZrO(NO_3)_2$ aqueous solution of 0.17 M was added drop-wise into NH_3 solution of 5 wt% with vigorously stirring and the final pH of the slurry was about 10. After ageing in the mother liquor at room temperature for 10 h, the formed white precipitate of $Zr(OH)_4$ was filtered and washed thoroughly with deionized water till the pH value of the filtered liquid was 7. The hydrogel was first divided into several parts. Some $Zr(OH)_4$ hydrogel was dried. One part of

* Corresponding author. Tel.: +86 21 64252041, fax: +68 21 64252041.
E-mail addresses: yqsong@mail.tsinghua.edu.cn (Y. Song), zj6083@yahoo.com.cn (J. Zhang), zyifei2001@yahoo.com.cn (Y. Zhang), xiaolong@ecust.edu.cn (X. Zhou), jwang@ipn.mx (J.-A. Wang), lyxu@dicp.ac.cn (L. Xu).

0920-5861/$ – see front matter © 2010 Elsevier B.V. All rights reserved.
doi:10.1016/j.cattod.2010.06.002

the dried $Zr(OH)_4$ was calcined in air at 400 °C, denoted as ZC and the other was impregnated with $Y(NO)_3$ and calcined at 550 °C, denoted as ZY (3% mol Y_2O_3). The remaining $Zr(OH)_4$ hydrogel was put into autoclave and subjected to the hydrothermal process at a given temperature for 24 h. The hydrothermal product was named as ZHt, where *t* represents the hydrothermal temperature. Part of ZH200 sample was calcined at 500 °C in air and the calcined sample was named as ZH200C. The tungstated zirconia was prepared by impregnating the hydrous zirconia with ammonium meta-tungstated and calcined at 700 °C in air for 3 h unless illustrated additionally. The calcined samples were denoted as WZC, WZY, WZHt and WZHtC. The content of tungsten oxide was 15 wt%. 0.5 wt% Pt was added to the obtained tungstated zirconia by impregnation with hexachloroplatinic acid solution and then calcined in air at 500 °C for 3 h. The samples containing Pt were denoted as PWZC, PWZY, PWZHt and PWZHtC.

2.2. Catalyst characterization

X-ray diffraction (XRD) patterns were obtained on a Philips MagiX X-ray diffractometer, using Cu $K\alpha_1$ radiation at room temperature and instrumental settings of 40 kV and 40 mA. The scanning was within a range of 2θ from 10° to 70° at a scanning rate of 6°/min.

H_2-temperature programmed reduction (H_2-TPR) was carried out on a TP5000 multi-functional adsorption equipment. The sample (0.1 g) was first pretreated in a flow of He at 400 °C for 30 min and then was cooled to room temperature. Subsequently, the sample was again heated from ambient temperature to 700 °C in a 5% H_2/N_2 flow (30 ml/min) at a heating rate of 10 °C/min.

NH_3-teperature programmed desorption (NH_3-TPD) was carried out at a home-made equipment. The sample (0.14 g) was loaded into a stainless steel U-shaped microreactor (i.d. = 5 mm) and pretreated at 600 °C for 0.5 h in flowing He. After the pretreatment, the sample was cooled down to 150 °C and was exposed to NH_3 atmosphere. As the catalyst is saturated with the adsorbed NH_3, helium was used as carrier to remove NH_3 physically adsorbed until the base-line was stable. NH_3-TPD was then carried out in a constant flow of He (20 ml/min) from 150 °C to 650 °C at a heating rate of 18 °C/min. The concentration of ammonia in the exit gas was monitored continuously by a gas chromatograph (Shimazu 8A) equipped with a TCD.

Raman spectra was obtained on Microscopic Confocal RM2000 Raman Spectrometer (Renishaw Corp.) equipped with the Lecia microscope at room temperature and atmospheric pressure. The magnification was 50. The exciting wavelength of 514.5 nm was generated with an Ar^+ laser with a power of 15 mW and a spot size of ca. 3 μm^2. The laser beam was focused on the top of the catalyst and the 25 different points on the each sample were analyzed. The acquisition time was 30.

2.3. Isomerization activity testing

The isomerization reaction of *n*-hexane (AR) was carried out in a continuous flow fixed-bed stainless steel reactor (i.d. = 5 mm). Before the reaction, the catalyst was pretreated in a flow of drying air at 450 °C for 3 h to remove the impurity such as hydrocarbon and water adsorbed on the catalyst surface. After that, the catalyst bed was cooled to 280 °C and reduced in a flow of hydrogen (20 ml/min) for 2 h. Subsequently, the temperature of the catalyst was decreased to a given value, and hydrogen and *n*-hexane were simultaneously introduced into the reactor. The molar ratio of H_2/*n*-hexane was 30, reaction pressure was 2 MPa, and weight hourly space velocity (WHSV) was 1 h^{-1}. The flow rate of *n*-hexane and hydrogen was controlled using a double column pump and a mass flow meter, respectively. The products were analyzed on-line by GC-920 (provided by Shanghai Institute of Computer Technology), equipped with an FID and an OV-101 capillary column.

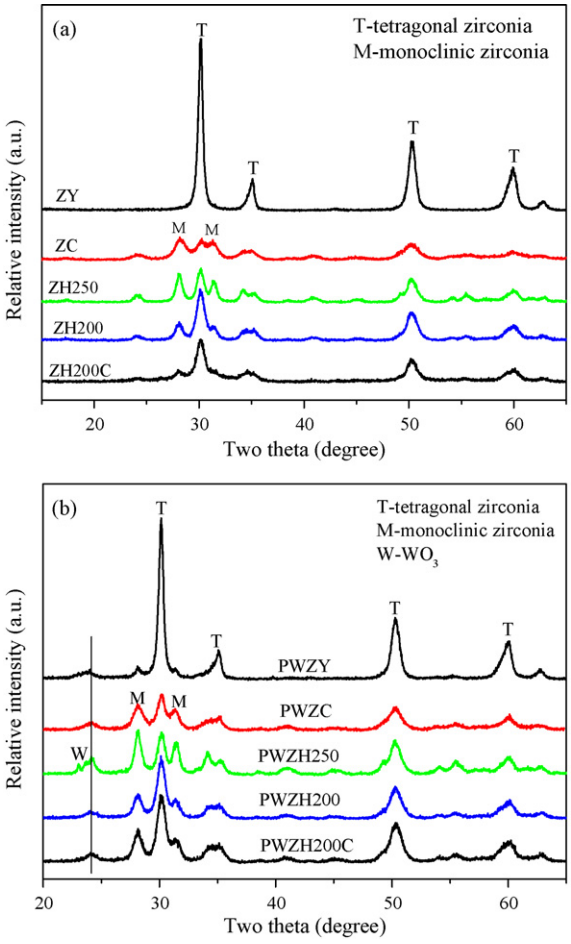

Fig. 1. XRD patterns of hydrous zirconia prepared by different methods and catalysts.

3. Results and discussion

3.1. Crystalline structure, surface area and pore structure

The XRD patterns of hydrous zirconia supports prepared by different methods are shown in Fig. 1a. Firstly, there appeared diffraction peaks at 28.1°, 31.4°, and 30.2° for ZC, corresponding to monoclinic phase and tetragonal phase (25%). In addition, the diffraction peaks of the sample were weak, which was indicative of low crystallization degree. The addition of Y led to the formation of complete tetragonal zirconia. Hydrous zirconia samples from hydrothermal process contained both tetragonal and monoclinic phases. The fraction of tetragonal phase in ZH200 was 66.5%, higher than that in ZH250 (25%), as shown in Table 2. The crystalline structure of ZC was similar to that ZH250 except that the crystallization degree of the former was lower than that of the latter. The calcination of ZH200 at 500 °C in air slightly altered the crystalline

Table 1
Acidity of different catalysts.

	PWZH200	PWZH250	PWZH200C	PWZY	PWZC
Total acid sites ($\mu mol/g_{cat}$)	3.00	2.85	2.71	2.28	3.22
Weak acid sites ($\mu mol/g_{cat}$)	1.69	1.65	1.48	1.15	2.06
Strong acid sites ($\mu mol/g_{cat}$)	1.31	1.20	1.23	1.13	1.16

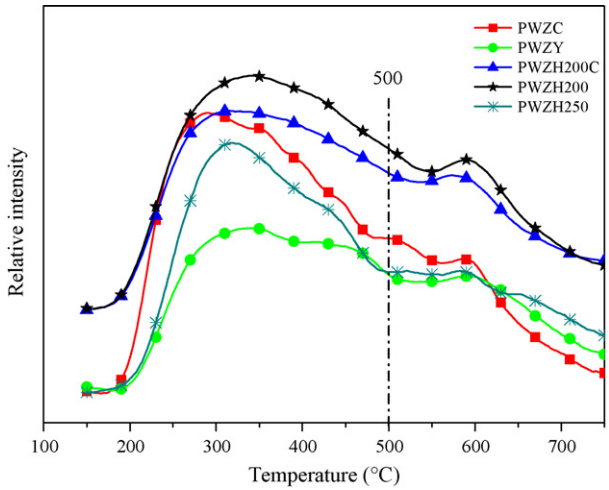

Fig. 2. NH_3-TPD profiles of different catalysts.

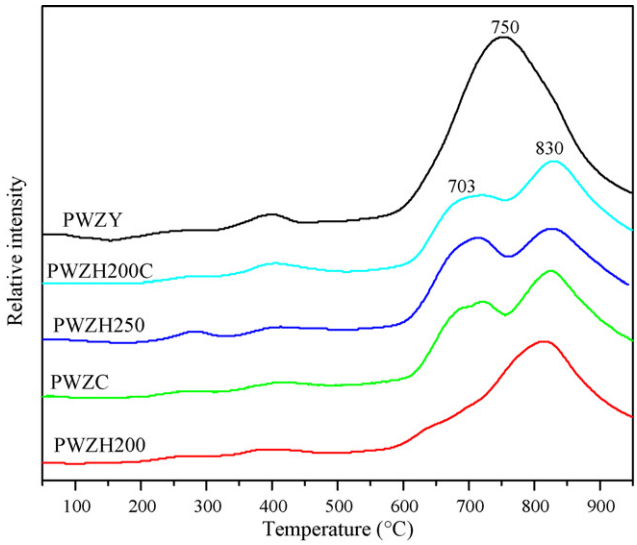

Fig. 3. H_2-TPR profiles of different catalysts.

phase composition and ZH200C contained 69% tetragonal zirconia. XRD patterns of the catalysts are shown in Fig. 1b. Obviously, tetragonal zirconia in PWZY was prominent (about 86.6%). The crystalline structures of PWZH200 and PWZH200C were very similar and the fraction of tetragonal zirconia in them was 55–57%, lower than that in PWZY. PWZH250 and PWZC also had similar crystalline structures and the fraction of tetragonal zirconia was lower, only 35–41%, compared with PWZH200. Additionally, there appeared diffraction peak of WO_3 in all samples and the diffraction peaks of WO_3 in PWZH250 was the strongest among the samples. This implied that WO_3 microcrystallites in PWZH250 were more than in other samples. In another words, more amorphous tungsten oxide existed in the samples except PWZH250.

As for the surface area of catalyst, the values of PWZH200, PWZH220C and PWZC was relatively similar, about 70 m^2/g_{cat}, which was higher than that of PWZH250 and PWZY. The average pore diameter of samples was roughly 9 nm except that the value for PWZC was smaller, only about 7 nm. The pore volume of samples ranged from 0.12 to 0.16 m^3/g_{cat}.

3.2. Acidity and reduction properties

The acidity of the catalyst was determined by NH_3-TPD and the results are shown in Fig. 2 and Table 1. The desorption peak at temperatures lower than 450 °C was considered to be related to the weak acid sties and that above the temperature to the strong acid sties. The desorption peak area represented the amount of acid sites. It could be seen from Table 1 that the amount of the total acid sites over PWZH200 was 3.00 μmol/g_{cat}, higher than that over different catalysts. Compared with PWZC and PWZY, the amount of the acid sites over PWZH250 and PWZH200C were relatively higher, about 2.7–2.8 μmol/g_{cat}. In addition, the strong acid sites over different catalysts decreased in the order: 1.31 μmol/g_{cat} for PWZH200 > ca. 1.2 μmol/g_{cat} for PWZH250 and PWZH200C > ca. 1.1 μmol/g_{cat} for PWZC and PWZY.

Table 2
BET surface area and pore structure of different catalysts.

	PWZH200	PWZH250	PWZH200C	PWZY	PWZC
S_{BET} (m^2/g_{cat})	73.5	58	72.2	51.5	75
Average pore diameter (nm)	9.4	9.9	8.8	9.2	7.1
Pore volume (m^3/g_{cat})	0.16	0.14	0.15	0.12	0.13
Tetragonal phase (%)[a]	66.5	39.5	69	100	25
Tetragonal phase (%)[b]	67.6	35	55	86.6	41

[a] Fraction of tetragonal phase in hydrous zirconia support.
[b] Fraction of tetragonal phase in Pt-promoted tungstated zirconia catalyst.

The reduction properties of the catalyst were characterized by H_2-TPR, as shown in Fig. 3. The reduction of pure WO_3 occurred at the temperature higher than 600 °C [4]. Three reduction peaks appeared at lower temperatures between 250 and 450 °C for the present Pt-promoted tungstated zirconia samples, which should be attributed to the introduction of ZrO_2 and Pt. In addition, two high temperature peaks between 600 and 900 °C, also appeared for all samples except that only one reduction peak appeared for PWZY. However, the reduction behaviors of different samples showed distinct difference. A very small reduction peak at ca. 660 °C and a very large one at 815 °C were observed in the TPR curve of PWZH200, while two large reduction peaks appeared in the TPR profiles of PWZ200C and PWZC, centering at 703 °C and 830 °C. The reduction at high temperature above 500 °C is generally considered to be related to the interaction strength between WOx and zirconia [6]. The higher the reduction temperature was, the stronger the interaction was. Therefore, the interaction between W and Zr over Pt/WZr-HT200 was the strongest among these catalysts.

3.3. Isomerization activity

Fig. 4 gives the isomerization activities of different catalysts (expressed as the yield of iso-hexanes). Apparently, the catalysts using crystalline hydrous zirconia as support prepared by different methods showed fairly different isomerization activities. The iso-hexanes yield over PWZH200 and PWZH250 could reach up to ca. 65% and 46% at 300 °C of the reaction temperature. The yield over PWZH200C was relatively low, only 35%. It is noteworthy that the yield of iso-hexanes over PWZY and PWZC was very low, only ca. 7%. That is to say, PWZY and PWZC hardly possessed isomerization activity. These results indicated that the crystalline hydrous zirconia prepared by hydrothermal method led to the catalyst with high catalytic activity.

3.4. Discussion

Although the effect of the preparation method of amorphous hydrous zirconia on the isomerization activity of Pt/WO_3–ZrO_2 was extensively investigated, the effect of the preparation method of crystalline hydrous zirconia was seldom reported. The present

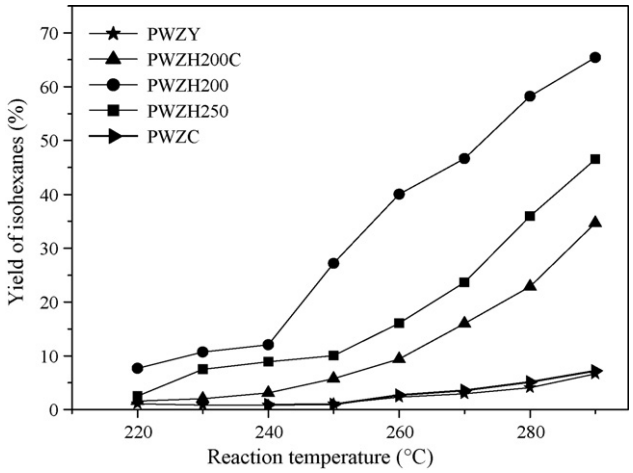

Fig. 4. Yield of iso-hexanes over different catalysts as a function of reaction temperature.

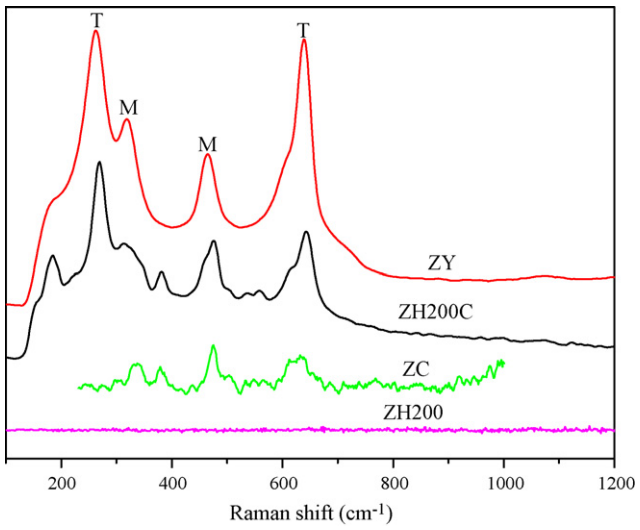

Fig. 5. Raman spectra of hydrous zirconia supports.

results showed that the catalyst using crystalline hydrous zirconia as support from hydrothermal method had higher catalytic activity than that from other methods. In order to clarify the reason for the effect of the preparation method on the isomerization activity, the possible correlations between physico-chemical properties of catalysts and catalytic activity were investigated. Firstly, for the role of the surface acidity of the catalyst, the amount of the strong acid sites over WZH200 was slightly more than that over other samples, but the isomerization activity of PWZH200 was much higher than that of others. Although PWZY and PWZC possessed the strong acid sites close to WZH200C and WZH250, the catalytic activity of the latter was much higher than that of the former. In fact, the former hardly had the isomerization activity. Therefore, it could be inferred that the presence of many strong acid sites was necessary, but insufficient to obtain the high isomerization activity. Vaudagna et al. [4,18,19] also considered that the catalytic activity was not dependent on the acidity.

Secondly, the effect of the phase compositions of the catalysts on the isomerization activity was also considered. The fraction of tetragonal zirconia in different catalysts is listed in Table 2. The fractions of tetragonal zirconia in PWZH200 and PWZH200C was very similar. Moreover, the support of the two catalysts also had the similar crystalline structures. But the activity of PWZH200 was much higher than that of PWZH200C. Besides, the activity of PWZH250 was also higher than that of PWZC although the fraction of tetragonal zirconia in the latter was a bit higher than in the former. Furthermore, Y-promoted support ZY consisted of complete tetragonal zirconia and the fraction of tetragonal zirconia in PWZY was the highest (86.6%) among the catalysts. Although tetragonal phase was generally considered to be active phase for isomerization reaction, the PWZY catalyst with more tetragonal phase zirconia exhibited the lowest catalytic activity. It seemed that the cyrstalline structure of support and zirconia in catalyst could not determine the isomerization activity, in agreement with the results from Houalla and coworkers [13,14]. In addition, they made a good correlation between the surface density of W atom on the catalyst and the catalytic activity and found that the suitable W surface atom density would be favorable to obtain the high isomerization activity. Additionally, Barton et al. [6] also indicated that the o-xylene isomerization activity of tungstated zirconia was related to the WO_x surface density. However, in the present investigation, the surface area of PWZH200 and PWZH200C was very similar and the W loading on the two samples was almost the same, so it could be reasonably inferred that the W surface atom density for the two samples should be comparable. Thus, the W surface atom density could not determine the catalytic activity of the studied catalysts. As for the crystalline phase of WO_3, all catalysts contained WO_3 microcrystallites. Although PWZH250 contained the most WO_3 microcrystallites, the catalytic activity was only intermediate. The content of WO_3 microcrystallites in PWZH200 and PWZH200C was comparable (evidenced by XRD in Fig. 1), but the former showed much higher catalytic activity than the latter. The above information implied that there must be other more important factor to control the catalytic activity.

In order to further elucidate the essence of the effect of the preparation method of crystalline hydrous zirconia on the catalytic activity, the hydrous zirconia samples were characterized by Raman spectrum, as shown in Fig. 5. No Raman band was observed for ZH200 and ZH250, but there appeared diffraction peaks for the two samples in XRD spectra (Fig. 1a). However, Raman bands representative of tetragonal and monoclinic phases were observed for ZC and ZY (Fig. 5), in line with the results in XRD spectra. Both bulk and surface structures of material are detected by XRD, while Raman spectrum is more sensitive to the surface region of material. Based on the above observations, it could be inferred that the surface region of ZH200 and ZH250 must be amorphous, while the inner layer of particles was crystallized. As for ZY and ZC prepared by the thermal treatment in air, the surface region were crystallized. The information allowed us to suggest that the hydrothermal method led to the crystallization of zirconium hydroxide only in the inner of the particles, while the thermal treatment in air led to the surface crystallization of particles. In order to confirm this point, ZH200 was calcined in air at 500 °C and the diffraction pattern of the obtained ZH200C was similar to that of the uncalcined samples ZH200 (Fig. 1a). However, the calcination in air resulted in obvious changes in Raman spectrum, i.e. there appeared Raman bands for ZH200C in Fig. 5, which confirmed that the thermal treatment in air could promote the crystallization of surface region of particles. Therefore, it could be inferred that the crystallization mode of $Zr(OH)_4$ would greatly influence the catalytic activity. The higher catalytic activity of PWZH200 and PWZH250 than PWZC and PWZY implied that the crystallization of particles inner from hydrothermal process led to high catalytic activity. On the contrary, the crystallization of surface region of particles in air resulted in a very low catalytic activity. Many investigations indicated that crystalline hydrous zirconia support led to an inactive catalyst [1,2,12], where the supports

were prepared by thermal treatment in air. However, the crystalline hydrous zirconia support from supercritical drying (in the absence of oxygen) led to a tungstated zirconia catalyst with high catalytic activity [15]. These results indirectly approved our proposal that the crystallization process of hydrous zirconia related to crystallization ambience has important influence on the catalytic activity.

To sum up, for the first time, the effect of crystallization mode of zirconium hydroxide which is related to treatment ambience of zirconium hydroxide on the isomerization activity of $Pt/WO_3–ZrO_2$ have been reported. In the absence of oxygen gas, the crystallization process (I) takes place only in the interior of $Zr(OH)_4$ particles, while the process (II) occurred on the surface region of the particles in the presence of oxygen. The crystalline hydrous zirconia from the process (I) led to a catalyst with high catalytic activity and the support from the process (II) resulted in an inactive catalyst.

Acknowledgements

We acknowledge the financial support of this work from Ministry of Science and Technology of P.R. China (Grant: 2004 CB 720603) and Postdoctoral Science Foundation of P.R. China (200902221).

References

[1] K. Arata, M. Hino, J. Chem. Soc., Chem. Commun. 18 (1988) 1259–1260.
[2] J.C. Yori, J.M. Parera, Catal. Lett. 65 (4) (2000) 205–208.
[3] Q.Y. Du, X.R. Chen, C.L. Chen, N.P. Xu, Chin. J. Catal. 27 (5) (2006) 397–402.
[4] S.R. Vaudagna, R.A. Comelli, N.S. Fígoli, Appl. Catal. A 164 (1) (1997) 265–280.
[5] J.C. Yori, C.R. Vera, J.M. Parera, Appl. Catal. A 163 (1) (1997) 165–175.
[6] D.G. Barton, S.L. Soled, G.D. Meitzner, G.A. Fuentes, E. Iglesia, J. Catal. 181 (1999) 57–72.
[7] S. Kuba, P. Lukinskas, R. Ahmad, F.C. Jentoft, R.K. Grasselli, B.C. Gates, H. Knözinger, J. Catal. 219 (2003) 376–388.
[8] R.A. Boyse, E.I. Ko, J. Catal. 171 (1997) 191–207.
[9] S.D. Rossi, G. Ferraris, M. Valing, D. Gazzoli, Appl. Catal. 231 (2002) 173–184.
[10] J.G. Santiesteban, D.C. Calabro, C.D. Chang, J.C. Vartuli, T.J. Fiebig, R.D. Bastin, J. Catal. 202 (2001) 25–33.
[11] S.D. Rossi, G. Ferraris, M. Valigi, D. Gazzoli, Appl. Catal. A 231 (2002) 173–184.
[12] D.G. Barton, S.L. Soed, G.D. Meitzner, G.A. Fuentes, E. Iglesia, J. Catal. 181 (1) (1999) 57–72.
[13] T. Onfroy, G. Clet, M. Houalla, J. Phys. Chem. B 109 (2005) 3345–3354.
[14] V. Lebarbier, G. Clet, M. Houalla, J. Phys. Chem. B 110 (2006) 13905–13911.
[15] Y.N. Huang, B.Y. Zhao, Y.C. Xie, Appl. Catal. A 172 (2) (1998) 327–331.
[16] M.A. Cortés-Jácome, J.A. Toledo, C. Angeles-Chavez, M. Agular, J.A. Wang, J. Phys. Chem. B 109 (48) (2005) 22730–22739.
[17] Y.Q. Song, C.L. Kang, Y.L. Feng, F. Liu, X.L. Zhou, R.Y. Dong, L.Y. Xu, Chin. J. Catal. 29 (12) (2008) 1196–1198.
[18] A. Martínez, G. Prieto, M.A. Arribas, P. Concepcíon, J.F. Sánchez-Royo, J. Catal. 248 (2) (2007) 288–302.
[19] M.A. Cortés-Jácome, C. Angeles-Chavez, E. Lopez-Salinas, J. Navareete, P. Toribio, J.A. Toledo, Appl. Catal. A 318 (1) (2007) 178–189.